ANALYTIC EXPRESSIONS FOR THE PROXIMITY ENERGY, THE FUSION PROCESS AND THE α EMISSION

R. MOUSTABCHIR AND G. ROYER

Rapport Interne SUBATECH 00-10

Analytic expressions for the proximity energy, the fusion process and the α emission

R. Moustabchir, G. Royer [1]

Laboratoire Subatech, UMR: IN2P3/CNRS-Université-Ecole des Mines, 4 rue A. Kastler, 44307 Nantes Cedex 03, France

Abstract

The entrance and exit channels through quasi-molecular shapes are compatible with the experimental data on fusion, light nucleus and α emissions when the proximity energy is taken into account. Analytic expressions allowing to determine rapidly this proximity energy are presented as well as formulas for the fusion barrier heights and radii and for the α emission barriers. Predictions for half-lives of exotic α emissions are proposed.

*PACS:*21.60.Ev; 23.60.+e; 21.10.Tg; 25.70.Jj
Keywords: Proximity energy; α emission; Half-lives; Fusion.

[1] E-mail:royer@subatech.in2p3.fr

1 Introduction

The possibility to synthetize superheavy elements by cold or warm fusion reactions [1–3] or using radioactive ion beams has renewed interest in investigating the fusion barriers. The only observed decay mode of these heaviest systems being the α emission an accurate description of the α decay is required. The pure Coulomb barrier sharply peaked at the touching point does not allow alone to determine correctly the fusion cross sections and the partial α decay half-lives. In the fusion path, the nucleon-nucleon forces act before the formation of a neck between the two quasi-spherical colliding ions and a proximity energy term must be added in the usual development of the liquid drop model [4]. Other nuclear potentials have also been developed to go beyond the Coulomb barrier [5,6]. It is highly probable that the α decay takes place also in this fusion-like deformation valley where the one-body shape keeps quasi-spherical ends while the transition between one and two-body configurations corresponds to two spherical nuclei in contact. Consequently, the proximity energy term plays also a main role to correctly describe the α decay barrier.
In previous works [7–9], this proximity energy term has been introduced in a generalized liquid drop model (GLDM) including also an accurate radius, the mass asymmetry and the temperature dependence. A quasi-molecular shape sequence has been defined to describe this fusion-like deformation valley. The fusion barrier heights and positions have been reproduced [10]. It has been shown that a degeneracy exists between the energy of elongated shapes where the proximity energy is negligible and the energy of compact and necked shapes which optimise the proximity energy. Consequently, this peculiar exit channel is also compatible with most of the fission data [9]: symmetric and asymmetric fission barrier heights, Businaro-Gallone point, fragment kinetic energies, partial half-lives for light nucleus emission [11] and even partial half-lives of α emission [12].
In a first work [13] analytic expressions reproducing some characteristics of the potential barriers derived from the GLDM have been proposed. In this work, other and simpler analytic formulas devoted to the proximity energy, the fusion barrier heights and positions and the α decay half-lives are presented. Finally, predictions for half-lives of exotic α emissions are proposed.

2 Energy of a deformed nucleus without neck

Within this GLDM the macroscopic total energy reads:

$$E(def) = E_V(def) + E_S(def) + E_C(def) + E_{Rot}(def). \qquad (1)$$

The moment of inertia, the quadrupole moment, the distance between the mass centres of the future fragments,... may be chosen as the deformation parameter. For one-body shapes, assuming volume conservation and constant density, the volume E_V, surface E_S and Coulomb E_C energies are given by:

$$E_V(MeV) = -15.494(1 - 1.8I^2)A(1 + 0.00337T^2), \tag{2}$$

$$E_S(MeV) = 17.9439(1 - 2.6I^2)A^{2/3}(S/4\pi R_0^2)(1 + 1.5T/17)(1 - T/17)^{3/2}, \tag{3}$$

$$E_C = 0.6e^2(Z^2/R_0) \times 0.5 \int (V(\theta)/V_0)(R(\theta)/R_0)^3 \sin\theta d\theta. \tag{4}$$

$I = (N - Z)/A$ is the relative neutron excess. The temperature dependence is needed to describe heavy-ion data at intermediate energies. S is the surface of the deformed nucleus. $V(\theta)$ is the electrostatic potential at the surface and V_0 the surface potential of the sphere.
The effective sharp radius R_0 has been chosen as:

$$R_0(fm) = (1.28A^{1/3} - 0.76 + 0.8A^{-1/3})(1 + 0.0007T^2). \tag{5}$$

This later formula proposed in Ref. [4] allows to reproduce the increase of the ratio $r_0 = R_0/A^{1/3}$ with the mass; for example, $r_0 = 1.10fm$ for ^{12}C and $r_0 = 1.18fm$ for ^{260}Lr.
For two separated spherical nuclei, these three contributions are given by:

$$E_V(MeV) = -15.494\left[(1 - 1.8I_1^2)A_1 + (1 - 1.8I_2^2)A_2\right](1 + 0.00337T^2), \tag{6}$$

$$E_S(MeV) = 17.9439\left[(1 - 2.6I_1^2)A_1^{2/3} + (1 - 2.6I_2^2)A_2^{2/3}\right] (1 + 1.5T/17)(1 - T/17)^{3/2}, \tag{7}$$

$$E_C = 0.6e^2Z_1^2/R_1 + 0.6e^2Z_2^2/R_2 + e^2Z_1Z_2/r, \tag{8}$$

where A_i,Z_i,R_i and I_i are the masses, charges, radii and relative neutron excesses of the two colliding nuclei or fragments. r is the distance between the mass centres.
Volume conservation leads to:

$$R_0^3 = R_1^3 + R_2^3. \tag{9}$$

When the two-body configurations play the main role, as in fusion reactions and α decay, R_1 and R_2 are determined from (5) and R_0 is derived from (9).

The discontinuity of a few MeV appearing at the contact point between the two spherical nuclei when Z_1/A_1 and Z_2/A_2 are very different has been substracted linearly from the contact point to the sphere to follow the progressive rearrangement of the nuclear matter.
The rotational energy has been determined within the rigid body ansatz.

$$E_{Rot} = \frac{\hbar^2 l(l+1)}{2I_\perp}. \tag{10}$$

3 Proximity energy in a neck or a gap

The surface energy E_S takes only into account the effects of the surface tension forces in a half space and does not include the contribution due to the attractive nuclear forces between the surfaces in regard in a neck or a gap between two colliding nuclei or two separated fragments. The nuclear proximity energy term E_{prox} has been introduced [4] to take into account these additional surface effects. However, in contrast to the frozen density picture and the connected approximations, in the GLDM the integration of the interaction energy between two similar flat surfaces in regard is effectively done in the neck or the gap and then depends explicitly on the selected shape sequence.

$$E_{prox}(r) = 2\gamma \int_{h_{min}}^{h_{max}} \Phi\left[D(r,h)/b\right] 2\pi h dh, \tag{11}$$

where h is the transverse distance varying from the neck radius for one-body shapes or zero for two-body configurations to the maximal transverse distance of the lighest part [8]. D is the distance between the opposite infinitesimal surfaces in regard and b the surface width fixed at 0.99 fm. Φ is the proximity function of Feldmeier [14]. The surface parameter γ is the geometric mean between the surface parameters of the two nuclei:

$$\gamma = 0.9517\sqrt{(1-2.6I_1^2)(1-2.6I_2^2)}\ MeV fm^{-2}. \tag{12}$$

In this approach the proximity energy is not connected to the surface diffuseness and the proximity energy vanishes when the neck fills up or when there is no neck as for ellipsoids for example.
This additional term in the usual development of the liquid drop model is essential as well in fusion as in fission studies; for example, at the contact point between two ^{100}Mo nuclei the proximity energy reaches -43 MeV and lowers the pure Coulomb Barrier by 35 MeV.

4 Analytic expressions for the proximity energy

The charge dependence of the proximity energy is included in the γ factor. For one-body shapes and within this adiabatic approach, the proximity energy depends on the shape sequence via the term D(r,h) and the range of integration. The part of the fusion-like deformation valley corresponding to one-body configurations has been described [8,9] by two halves of different elliptic lemniscatoids joined at a distance a of the deformation axis (see fig.1). Namely:

$$R(\theta)^2 = \begin{cases} a^2 sin^2\theta + C_1^2 cos^2\theta, 0 \leq \theta \leq \frac{\pi}{2} \\ a^2 sin^2\theta + C_2^2 cos^2\theta, \frac{\pi}{2} \leq \theta \leq \pi. \end{cases} \tag{13}$$

Assuming volume conservation and connecting the two elongations C_1 and C_2 ($C_2 \leq C_1$) by

$$C_2^2 = a^2 + (C_1^2 - a^2)\beta^2, \tag{14}$$

where $\beta = \frac{R_2}{R_1}$, the whole shape sequence from two touching spherical nuclei ($a = 0$) to a spherical nucleus ($a = C_1 = C_2$) is simulated, the adiabatic formation of a deep neck and its progressive filling taking place naturally while keeping almost spherical ends.
Then, the distance between the elements of surface is

$$D(r,h) = D_1(h) + D_2(h) + S_{eff}(r), \tag{15}$$

where

$$D_i(h) = \sqrt{\frac{1}{2}C_i^2 - h^2 - (\frac{1}{4}C_i^4 - h^2 C_i^2(1 - \frac{a^2}{C_i^2}))^{1/2}} \; (i = 1,2). \tag{16}$$

The separation S_{eff} betwen the effective surfaces is taken as

$$S_{eff}(r) = r - C_1^{eff} - C_2^{eff}, \tag{17}$$

where $C_i^{eff} = R_i - b^2/2R_i$ is the mean between the central radii of the density and potential distributions.
The transverse distance h varies from a (0 for two separated spherical nuclei) to the maximum $h_{max} = \frac{C_2}{2\sqrt{1-(\frac{a}{c_2})^2}}$.

For one-body shapes, only very complicated analytical formulas can be deduced from the integration formula (11). A fitting procedure adjusted on

around 300 symmetric and very asymmetric systems has been prefered. It leads to the following expression ($A_1 > A_2$) with a rms deviation from the values deduced from the GLDM of $0.26MeV$.

$$\frac{E_{prox}(MeV)}{4\pi\gamma} = 0.485 + e^{-0.76(R_1+R_2-r)}[-0.09035A_1 - 0.06895A_2 - 8.953.10^{-6}A_1^{1/3}A_2^{1/3}r^4 + \frac{A_1^{1/3}A_2^{2/3}(3.1777 - \frac{18.522A_1^{1/3}}{r^2})}{A_1^{1/3}+A_2^{1/3}} + \frac{0.2032A_1^2 - 0.35147A_2^2 + 4.688(A_1A_2^{1/3} + A_1^{1/3}A_2)}{r^3} - \frac{1.65164A_1^{1/3}A_2^{2/3}r}{A_1^{2/3}+A_2^{2/3}} + (\frac{0.12607A_2^{1/3}}{A_1^{1/3}} + 0.005013A_1^{1/3}A_2^{1/3})r^2 - 0.1982\sqrt{A_1^{2/3} - A_2^{2/3}}(R_1+R_2-r)^2]. \quad (18)$$

For two separated spherical nuclei, the proximity energy can be calculated with the simpler following formula with a rms deviation of $0.23MeV$

$$E_{prox}(MeV) = 4\pi\gamma\frac{C_1^{eff}C_2^{eff}}{C_1^{eff}+C_2^{eff}} \left[\frac{-0.0527}{0.025e^{0.12(r-(C_1^{eff}+C_2^{eff}))} + 0.0085e^{1.52(r-(C_1^{eff}+C_2^{eff}))}} + \frac{1.956}{r^2} - \frac{0.142}{r}\right] \quad (19)$$

As an example, these two sheets forming the proximity energy are vizualized in fig. 2 when the heavier nucleus is ^{208}Pb.
For the α emission where the proximity energy between the two separated α particle and daughter nucleus plays the central role a very accurate formula has been obtained ($rms = 0.06MeV$)

$$E_{prox}(MeV) = (4\pi\gamma)e^{-1.38(r-R_\alpha-R_d)} \left[0.6584A^{2/3} - (\frac{0.172}{A^{1/3}} + 0.4692A^{1/3})r - 0.02548A^{1/3}r^2 + 0.01762r^3\right], \quad (20)$$

where A is the mass of the mother nucleus and r the mass-centre distance. To obtain the α decay barrier from the contact point between the nascent α particle and daughter nucleus it is sufficient to add at this proximity energy displayed in Fig. 3 the Coulomb repulsion.

5 Formulas for the fusion barrier height and radius

For low and moderate energies and for light and medium systems the fusion process depends only on the fusion barrier height and position and, therefore, strongly on the sum of the nuclear proximity and Coulomb energies [5,15]. Indeed, the top of the barrier lies well outside the contact point and once the saddle point has been passed, the nuclear system fuses automatically. To explain the fusion of very heavy nuclear systems, fusion of light and medium systems at high energies and sub-barrier fusion it is necessary to advocate also double-humped fusion barriers, dissipative forces, neck formation and coupled-channel effects [8,10,16,17].
Two new formulas given the fusion barrier height and radius are proposed here from a fitting procedure on GLDM data on 170 fusion reactions. The rms deviations are respectively $0.15MeV$ and $0.08fm$.

$$E_{0,fus} = -19.38 + \frac{2.1388Z_1Z_2 + 59.427(A_1^{1/3} + A_2^{1/3}) - 27.07\ln(\frac{Z_1Z_2}{A_1^{1/3}+A_2^{1/3}})}{(A_1^{1/3} + A_2^{1/3})(2.97 - 0.12\ln(Z_1Z_2))}, \quad (21)$$

$$R_{0,fus}(fm) = (A_1^{1/3} + A_2^{1/3})\left[1.908 - 0.0857ln(Z_1Z_2) + \frac{3.94}{Z_1Z_2}\right]. \quad (22)$$

Theoretical fusion barrier heights $E_{0,fus}$ and empirical data are compared in the whole mass and asymmetry range in Table 1. The predictions of the GLDM agree with the experimental data. The formula (21) reproduces the GLDM data more precisely than the formula (19) previously proposed in Ref. [13] and with the same accuracy than the much longer polynomial expression already given (formula (21) in [13]). The preceding formulas lead to higher barrier heights than the ones derived from the Bass potential [5] for the heaviest nuclei, as experimentally observed apparently [1,19].

6 α decay barrier

The α decay barrier consists of two very distinct parts. The first one around the sphere before the rupture of the matter bridge between the emitted fragments is strongly model dependent. It can be described by the GLDM or parabolic, cubic,.. approximations. Its contribution to the α decay half-life is negligible since the deformation energy is very close to zero or even negative and since the distance between the mass centres increases only slightly [12]. For example, for a ^{108}Te nucleus r varies from 4.9 to 7.2 fm while the outer point of the tunneling process takes place at 41.9 fm. The second external part corresponds to two separated spheres and is much more straightforward. Its

energy is completely defined by the sum of the usual Coulomb repulsion and the proximity energy given accurately by the formula (20). The problem is not to discuss either the entrance point of the tunneling process is the initial sphere or the contact point since the deduced half-lives will be almost identical but to respect the experimental Q_α value at the sphere which must have the same energy than the outer point defined by $r_{out} = e^2 Z_\alpha Z_d / Q_\alpha$. As an example, the total deformation energy for the α emission of ^{108}Te and its two constituents are displayed in Fig. 4. It has been shown recently [12] that these potential barriers allow to determine accurately the α decay half-lives within the WKB barrier penetration probability and without preformation factor.

7 Expressions for the α decay half-lives

A fitting procedure on 373 α emitters having an α branching ratio close to one has led to the following formulas respectively for the even-even, even-odd, odd-even and odd-odd nuclei . A and Z are the mass and charge of the mother nucleus. The rms deviation are respectively 0.285, 0.39, 0.36 and 0.35.

$$log_{10}\left[T_{1/2}(s)\right] = -25.31 - 1.1629 A^{1/6}\sqrt{Z} + \frac{1.5864 Z}{\sqrt{Q_\alpha}}, \tag{23}$$

$$log_{10}\left[T_{1/2}(s)\right] = -26.65 - 1.0859 A^{1/6}\sqrt{Z} + \frac{1.5848 Z}{\sqrt{Q_\alpha}}, \tag{24}$$

$$log_{10}\left[T_{1/2}(s)\right] = -25.68 - 1.1423 A^{1/6}\sqrt{Z} + \frac{1.592 Z}{\sqrt{Q_\alpha}}, \tag{25}$$

$$log_{10}\left[T_{1/2}(s)\right] = -29.48 - 1.113 A^{1/6}\sqrt{Z} + \frac{1.6971 Z}{\sqrt{Q_\alpha}}. \tag{26}$$

8 α decay half-lives of "exotic" nuclei

The preceding formulas have been obtained for known nuclei for which the α decay is the main decay mode. In Table 2 the values obtained with these different analytic expressions are compared with the experimental data for nuclei for which Q_α is only extrapolated [20] and the α branching ratio is very different of one. Taking into account the uncertainties on Q_α and the branching ratio, the agreement is quite correct.
From this result, predictions for still less known nuclei and α decays are given in Table 3. The experimental uncertainties are still rather large. These theoretical values might be useful to estimate the α decay branching ratio.
Recently [21], the α decay of the new isotopes ^{188,189}Po has been observed. The

experimental values of $log_{10}\left[T_{1/2}(s)\right]$ are -3.4 for ^{188}Po ($Q_\alpha = 8.087MeV$) and -2.3 for ^{189}Po ($Q_\alpha = 7.703MeV$). The GLDM gives respectively -4.1 and -3.0 while the formulas (23-26) lead to -4.0 and -2.5. This confirms the efficiency of the GLDM and justifies the utilization of these analytic formulas for 'exotic' nuclei.

9 Summary and conclusion

Recent studies have shown that the entrance and exit channels through one and two-body quasi-molecular shapes are compatible with the experimental data on fusion, fission, light nucleus and α emissions when the proximity energy is taken into account within a generalized liquid drop model including also an accurate nuclear radius and the mass asymmetry.
Different analytic expressions allowing to determine rapidly the proximity energy in this deformation path and, therefore, the fusion and α decay barriers are presented here as well as formulas for the fusion barrier heights and radii and for the α emission. Predictions for half-lives of exotic α emissions are also proposed.

References

[1] S. Hofmann and G. Munzenberg, GSI report 2000-02 (2000).

[2] P. Armbruster, E. Phys. J. A 7 (2000) 23.

[3] Y.T. Oganessian et al, Phys. Rev. Lett. 83 (1999) 3154.

[4] J. Blocki, J. Randrup, W.J. Swiatecki and C.F. Tsang, Ann. of Phys. 105 (1977) 427.

[5] R. Bass, Proc. Conf. on deep inelastic and fusion reactions with heavy ions, Berlin 1979, (Springer) p 281.

[6] H. Ngo and C. Ngo, Nucl. Phys. A 348 (1980) 140.

[7] G. Royer and B. Remaud, J. Phys. G 10 (1984) 1057.

[8] G. Royer and B. Remaud, Nucl. Phys. A 444 (1985) 477.

[9] G. Royer, in: Heavy Elements and Related New Phenomena, ed. R. K. Gupta and W. Greiner (World Scientific, 1999) p 591.

[10] G. Royer, J. Phys. G 12 (1986) 623.

[11] G. Royer, R.K. Gupta and V.Y. Denisov, Nucl. Phys. A 632 (1998) 275.

[12] G. Royer, J. Phys. G (2000) in print.

[13] G. Royer, C. Normand and E. Druet, Nucl. Phys. A 634 (1998) 267.

[14] H. Feldmeier, 12th Summer School on Nuclear Physics, Mikolajki, Poland, 1979.

[15] L.C. Vaz, J.M. Alexander and G.R. Satchler, Phys. Reports 69 (1981) 373.

[16] W.J. Swiatecki, Nucl. Phys. A 376 (1982) 275.

[17] R. Lindsay and N. Rowley, J. Phys. G 10 (1984) 805.

[18] G. Royer and C. Piller, J. Phys. G 18 (1992) 1805.

[19] G. Royer, R. Moustabchir and R.A. Gherghescu, Proc. Int. Conf. on Nuclear Reaction Mechanisms, Varenna, Italy, 2000, ed. Ricerca Scientifica ed Educazione Permanente (Universita Di Milano) in print.

[20] G. Audi, O. Bersillon, J. Blachot and A. H. Wapstra, Nucl. Phys. A 624 (1997) 1.

[21] A.N. Andreyev et al, Eur. Phys. J. A 6 (1999) 381.

Figure captions

Fig. 1. Shape characteristics in the deformation path through compact quasi-molecular configurations.

Fig. 2. Proximity energy (divided by $4\pi\gamma$) between a ^{208}Pb nucleus and a nucleus of mass A_2 as a function of the mass-centre distance.

Fig. 3. Proximity energy (divided by $4\pi\gamma$) between two nascent separated α particle and daughter spherical nucleus coming from a mother nucleus of mass A.

Fig. 4. Coulomb and proximity energies and total deformation energy (potential barrier) after the separation point for the α emission of ^{108}Te. r is the mass-centre distance. The zero energy at the sphere is adjusted to reproduce the experimental Q_α value.

Table captions

Table 1. Comparison of empirical, theoretical and analytic fusion barrier heights. The references of the empirical data (column 2) are given in Refs. [8,10,18]. The values derived from the GLDM are given in the third column. The fourth, fifth and last columns correspond respectively to the formula (21) of the present work and the formulas (19) and (21) in Ref. [13].

Table 2. Comparison between the experimental value of $log_{10}\left[T_{1/2}(s)\right]$ and the theoretical one obtained with the formulas (23-26) for nuclei having either a small α branching ratio or only an extrapolated mass in Ref. [20].

Table 3. GLDM predictions for the half-lives of nuclei having either a small α branching ratio or only an extrapolated mass in [20] and for which only a lower or higher limit of the half-life is known experimentally.

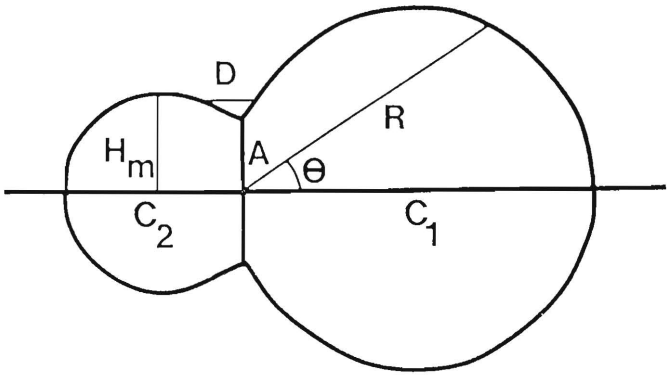

Figure 1

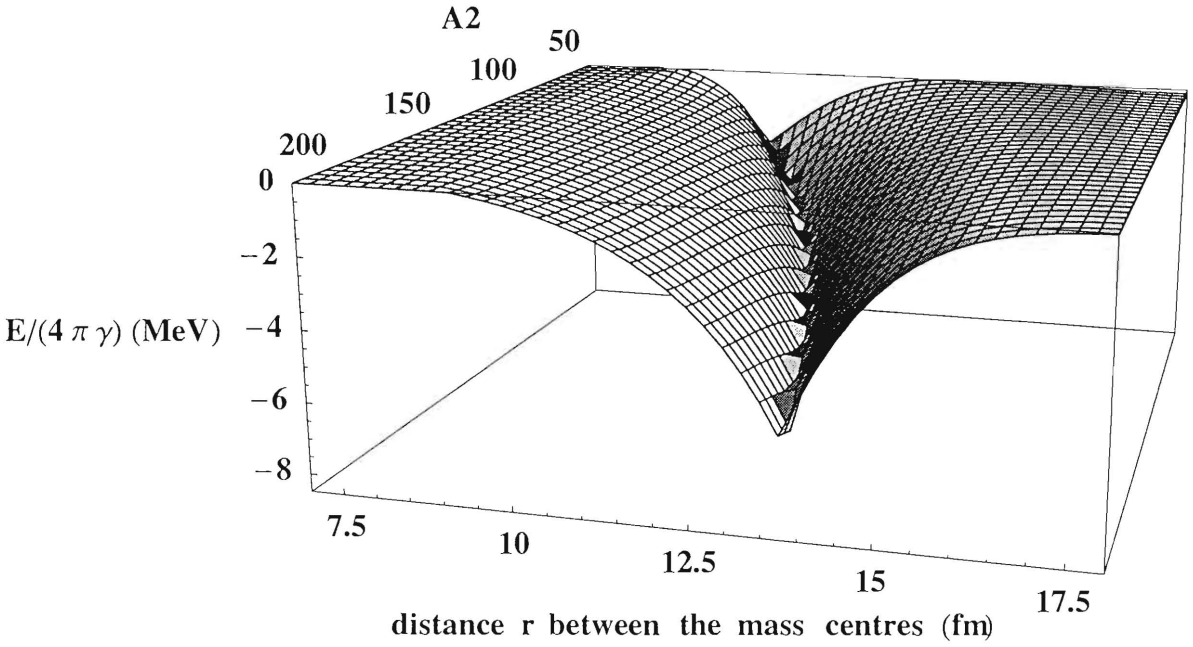

Figure 2

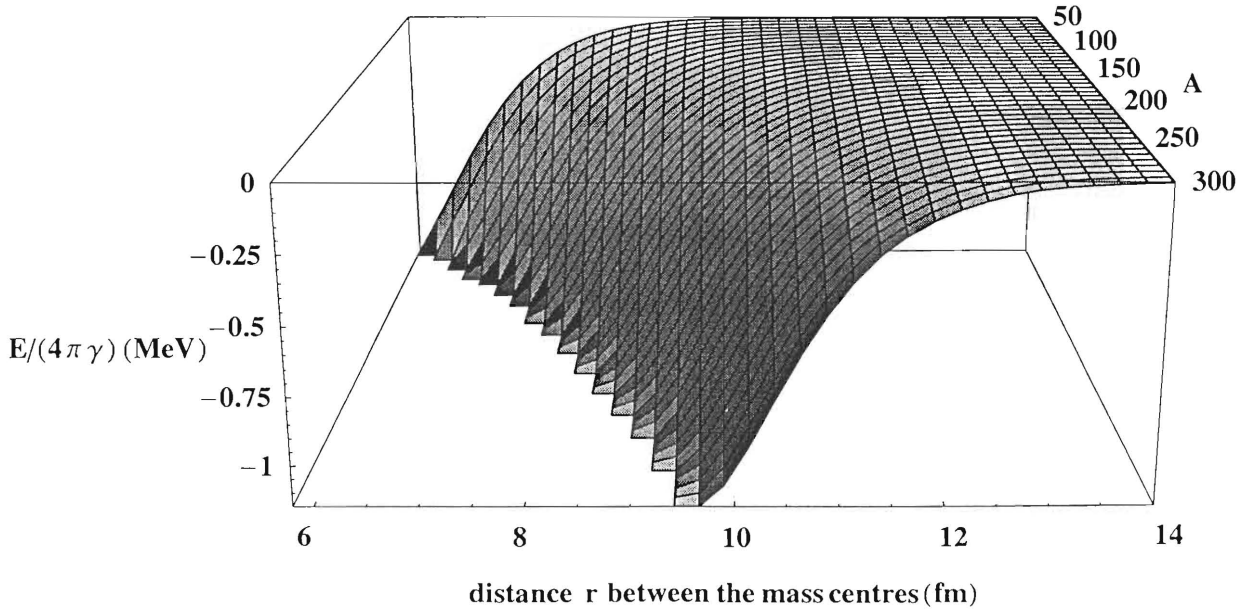

Figure 3

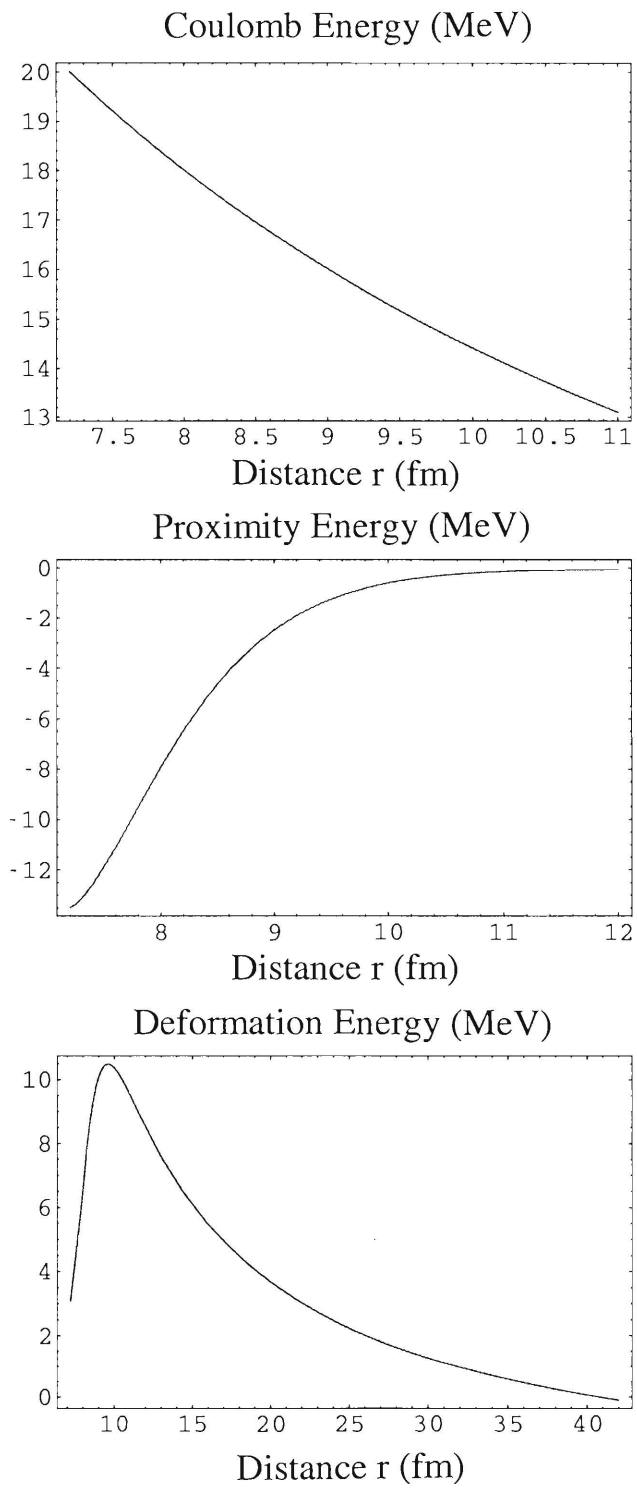
Coulomb Energy (MeV)
20
19
18
17
16
15
14
13
7.5
8
8.5
9
9.5
10
10.5
11
Distance r (fm)
Proximity Energy (MeV)
0
-2
-4
-6
-8
-10
-12
8
9
10
11
12
Distance r (fm)
Deformation Energy (MeV)
10
8
6
4
2
0
10
15
20
25
30
35
40
Distance r (fm)

Figure 4

Table 1

Reaction	$E_{0,fus}$ (MeV) (Empirical)	$E_{0,fus}$ (MeV) (GLDM)	$E_{0,fus}$ (MeV) expression (21)	$E_{0,fus}$ (MeV) expression (19) in [13]	$E_{0,fus}$ (MeV) expression (21) in [13]
$^{12}C + ^{10}B$	5.24	5.03	4.91	5.02	5.02
$^{4}He + ^{44}Ca$	6.37	6.20	6.44	5.99	6.49
$^{14}N+^{14}N$	8.17	8.01	7.85	7.96	7.91
$^{4}He + ^{59}Co$	8.26	8.10	8.40	7.79	8.43
$^{12}C + ^{27}Al$	12.29	12.24	12.16	12.13	12.22
$^{24}Mg+^{24}Mg$	21.53	21.88	21.79	21.94	21.91
$^{32}S + ^{24}Mg$	27.93	28.48	28.4	28.73	28.52
$^{28}Si+^{28}Si$	28.95	29.04	28.97	29.33	29.09
$^{30}Si+^{30}Si$	28.1	28.4	28.49	28.67	28.45
$^{32}S + ^{27}Al$	29.89	30.47	30.44	30.81	30.55
$^{12}C + ^{110}Pd$	35.1	36.59	36.72	36.70	36.59
$^{16}O + ^{144}Sm$	59.9	62.29	62.23	63.51	62.34
$^{40}Ca + ^{58}Ni$	73.36	74.72	74.52	77.03	74.62
$^{35}Cl + ^{90}Zr$	84.87	86.50	86.41	89.1	86.4
$^{16}O + ^{238}U$	83.2	84.70	84.50	86.14	85.79
$^{58}Ni+^{58}Ni$	97.9	100.6	100.4	103.6	100.5
$^{64}Ni+^{64}Ni$	93.5	97.32	97.43	100.3	97.34
$^{40}Ar + ^{112}Sn$	109.1	109.5	109.5	112.4	109.6
$^{86}Kr + ^{62}Ni$	119.3	121.4	121.45	124.2	121.4
$^{74}Ge+^{74}Ge$	120.8	123.1	123.15	125.9	123.0
$^{40}Ar +^{148}Sm$	129.4	130.3	130.25	132.3	130.3
$^{86}Kr + ^{70}Ge$	136.5	137.2	137.2	139.4	137.2
$^{40}Ar + ^{165}Ho$	141.4	138.4	138.35	139.9	138.3
$^{37}Cl + ^{209}Bi$	156.2	157.2	157.0	156.7	157.2
$^{81}Br + ^{104}Ru$	174.0	176.2	176.3	174.9	176.2
$^{90}Zr + ^{90}Zr$	182.0	184.8	184.8	182.7	184.8
$^{90}Zr + ^{96}Zr$	184.5	182.8	182.9	180.8	182.9
$^{96}Zr + ^{96}Zr$	181.4	180.9	181.1	180.8	180.8
$^{40}Ar + ^{238}U$	185.0	179.3	179.2	175.9	179.3
$^{100}Mo +^{90}Zr$	195.9	191.2	191.2	187.9	191.2
$^{100}Mo+^{100}Mo$	207.2	197.8	198.0	193.2	197.8
$^{54}Cr + ^{196}Os$	203.5	198.8	198.8	192.9	198.8
$^{86}Kr + ^{123}Sb$	209.4	204.1	204.3	198.2	204.1
$^{48}Ca+^{248}Cm$	210.0	203.1	203.2	195.4	203.1
$^{124}Sn + ^{94}Zr$	219.5	219.9	220.15	210.9	219.9
$^{58}Fe + ^{209}Bi$	236.5	232.1	232.1	219.3	232.3
$^{76}Ge + ^{170}Er$	237.0	234.6	234.8	221.6	234.7

Table 2

nuclide	Q_α (MeV)	$\log_{10}[T_{1/2,\ \alpha,\ exp}(s)]$	$\log_{10}[T_{1/2,\ \alpha,\ theo}(s)]$
^{106}Te	4.295	-4.15	-3.75
^{112}I	2.985	5.45	4.79
^{113}I	2.711	9.3	7.28
^{115}Xe	2.625	6.78	8.57
^{158}Yb	4.171	6.63	6.44
^{158}Lu	4.785	3.06	3.80
^{158}W	6.595	-3.0	-2.86
^{159}Lu	4.488	4.48	5.27
^{159}W	6.445	-2.0	-2.2
^{160}Hf	4.905	3.29	3.27
^{160}W	6.07	-0.99	-0.97
^{160}Re	6.695	-2.06	-2.75
^{161}W	5.915	-0.25	-0.22
^{162}Ta	5.005	3.68	3.69
^{162}Re	6.275	-0.94	-1.17
^{162}Os	6.785	-2.77	-2.69
^{163}Ta	4.755	3.74	4.8
^{163}Re	6.015	0.09	-0.12
^{163}Os	6.675	-2.26	-2.16
^{164}Re	5.925	-0.04	0.26
^{166}Ir	6.705	-1.95	-1.91
^{167}Re	5.255	0.53	3.19
^{167}Ir	6.495	-0.49	-1.1
^{169}Re	5.035	5.21	4.27
^{171}Pt	6.605	-1.42	-1.15
^{174}Ir	5.625	3.25	2.54
^{175}Ir	5.715	3.02	1.89
^{175}Au	6.675	-0.62	-1.01
^{175}Hg	7.045	-1.92	-1.85
^{176}Ir	5.235	2.58	4.51
^{177}Ir	5.125	4.7	4.72
^{179}Tl	6.815	≈ - 4.72	-6.9
^{180}Hg	6.265	0.73	0.68
^{180}Tl	6.815	-2.3	-0.62
^{182}Au	5.525	4.07	4.01
^{183}Tl	6.225	2.54	1.51
^{183}Pb	7.025	-0.5	-1.05
^{185}Pt	4.535	7.93	8.5
^{185}Hg	5.775	2.91	2.92
^{185}Pb	6.675	0.61	0.81
^{186}Au	4.905	7.9	7.42
^{187}Au	4.795	7.22	7.48
^{188}Hg	4.715	10.72	8.24
^{188}Pb	6.115	2.48	2.09
^{190}Pb	5.695	3.9	3.95
^{190}Bi	6.855	0.91	0.008
^{190}Po	7.635	-2.77	-2.64

^{191}Po	7.475	-1.77	-1.84
^{192}Pb	5.215	6.54	6.36
^{193}At	7.535	-1.4	-1.7
^{194}Pb	4.735	9.99	9.13
^{194}At	7.315	-1.4	-0.83
196Bi	5.465	7.42	6.34
196Rn	7.625	-2.39	-1.89
197Bi	5.385	8.75	6.16
^{197}Rn	7.415	-1.18	-0.89
^{200}Fr	7.625	-1.62	-1.11
^{201}Fr	7.535	-1.21	-1.01
^{203}Bi	4.148	11.63	13.97
^{203}Ra	7.735	-2.4	-1.2
^{204}Ra	7.635	-1.22	-1.25
^{207}Ac	7.865	-1.38	-1.37
^{210}Bi	5.036	11.52	8.57
^{210}Po	5.407	7.08	6.01
^{210}At	5.631	7.22	6.29
^{210}Fr	6.7	2.5	2.25
^{211}Bi	6.75	2.11	-0.21
^{211}Po	7.594	-0.29	-2.62
^{212}At	7.828	-0.5	-2.98
^{212}Fr	6.529	3.45	2.95
^{212}Th	7.955	-1.44	-1.63
^{213}Bi	5.982	5.12	2.91
^{213}Rn	8.243	-1.6	-3.79
^{213}Fr	6.905	1.54	0.99
^{214}Fr	8.588	-2.3	-4.49
^{214}Pa	8.275	-1.77	-1.76
^{215}Ra	8.864	-2.8	-4.74
^{216}Ac	9.243	-3.48	-5.52
^{218}Ac	9.379	-5.97	-5.92
^{218}Pa	9.795	-3.935	-6.18
^{218}U	8.785	-2.22	-3.43
^{219}U	9.865	-4.26	-5.8
^{220}At	6.045	3.44	3.98
^{220}Ac	8.346	-1.58	-3.0
^{220}Pa	9.831	-6.11	-6.31
^{222}U	9.496	-5.85	-5.39
^{223}U	8.935	-4.68	-3.52
^{224}Ac	6.327	5.06	4.69
^{224}U	8.62	-3.02	-3.09
^{225}U	8.018	-1.03	-0.84
^{226}Ac	5.536	9.25	8.8
^{226}U	7.715	-0.82	-0.29
^{226}Np	8.195	-1.46	-0.84
^{227}Th	6.146	6.21	5.44
^{227}Np	7.815	-0.29	0.07
^{228}Ac	4.825	11.6	13.33
^{228}Pa	6.265	6.63	5.98
^{228}Np	7.415	2.17	1.95

^{230}Pa	5.439	9.29	10.46
^{231}Th	4.213	14.96	17.32
^{231}Pa	5.15	12.01	11.17
^{232}Np	6.014	7.47	8.27
^{232}Am	7.275	3.59	3.4
^{234}Am	6.875	5.55	5.08
^{236}Np	5.006	15.48	14.38
^{240}Bk	7.065	3.46	5.13
^{243}Bk	6.875	7.03	5.11
^{243}Fm	8.695	-0.46	-0.03
^{244}Bk	6.778	8.42	6.35
^{244}Es	8.025	2.87	2.15
^{244}Fm	8.545	-0.48	-0.11
^{250}Md	8.305	2.87	1.92
^{250}No	8.955	-0.30	-0.71
^{251}Bk	5.646	10.52	11.05
^{252}Lr	9.145	0.05	0.06
^{253}Es	6.739	6.25	6.45
^{253}Lr	8.985	0.22	-0.13
^{253}Rf	9.545	-1.58	-1.15
^{254}Cf	5.927	9.23	9.58
^{254}Es	6.615	7.38	7.98
^{254}Lr	8.845	1.22	0.87
^{254}Rf	9.375	-2.11	-1.27
^{255}Cf	5.734	10.71	11.14
^{255}Md	7.907	4.31	2.59
^{255}Rf	9.245	0.49	-0.33
^{255}Db	9.715	0.33	-1.52
^{256}Cf	5.555	10.87	11.64
^{256}Md	7.895	4.63	3.34
^{257}Md	7.558	5.12	3.86
^{257}Lr	9.055	-0.19	-0.42
^{257}Rf	9.145	0.77	-0.07
^{257}Db	9.315	0.23	-0.42
^{258}Md	7.272	6.65	5.86
^{258}No	8.147	2.08	1.75
^{258}Rf	9.327	-1.03	-1.21
^{258}Db	9.545	0.86	-0.58
^{259}Rf	9.12	0.46	-0.03
^{259}Sg	9.835	-0.19	-1.31
^{260}Rf	8.898	0.002	0.04
^{261}Sg	9.805	-0.62	-1.26
^{261}Bh	10.335	-1.86	-2.56
^{262}Db	9.005	2.12	1.05
^{263}Rf	8.305	3.3	2.51
^{263}Db	10.665	-3.0	-2.8

Table 3

nuclide	Q_α (MeV)	$\log_{10}[T_{1/2,\,\alpha,\,exp}(s)]$	$\log_{10}[T_{1/2,\,\alpha,\,theo}(s)]$
^{109}I	3.785	> -1.7	-0.49
^{114}Ba	3.595	> 2.13	2.38
^{119}Cs	1.724	> 9.33	22.22
^{120}Cs	1.247	> 8.49	35.77
^{150}Tb	3.587	> 7.4	8.08
^{152}Tb	3.084	> 12.95	12.6
^{160}Lu	4.105	> 8.56	8.14
^{163}Hf	4.005	> 7.6	8.83
^{165}W	5.035	> 3.4	3.74
^{165}Os	6.325	< -0.92	-0.93
^{170}W	4.125	> 4.16	8.95
^{170}Re	4.745	> 4.96	6.26
^{173}Ir	5.845	> 2.11	1.36
^{177}Au	6.435	>0.47	-0.16
^{178}Au	6.115	< 0.81	1.27
^{180}Au	5.855	<2.65	1.27
^{182}Tl	6.555	> 1.7	0.36
^{186}Tl	5.895	> 7.52	3.2
^{187}Re	1.653	> 24.14	43.53
^{187}Hg	5.075	< 7.98	6.4
^{187}Bi	7.605	< -1.15	-2.65
^{189}Au	4.375	> 7.98	10.13
^{189}Hg	4.445	> 9.18	10.22
^{189}Bi	7.265	< 0.13	-1.59
^{190}Au	3.86	> 11.41	15.04
^{190}Hg	3.955	> 9.38	13.57
^{192}Hg	3.328	> 11.64	19.28
^{193}Au	2.619	> 11.8	27.63
^{194}Tl	3.498	> 12.3	19.92
^{196}Pb	4.225	>9.87	12.6
^{198}At	6.895	< 0.65	0.68
^{201}Bi	4.505	> 9.81	11.39
^{202}Pb	2.598	> 14.28	29.89
^{202}Bi	4.285	> 10.79	14.00
^{217}Po	6.665	< 0.19	0.52
^{225}Np	8.785	> -5.7	-2.89
^{228}Pu	7.945	> -5.7	-0.27
^{229}Pu	7.595	> -5.7	1.36
^{230}Np	6.776	<3.96	4.58
^{238}Cm	6.617	>4.94	5.53
^{240}U	7.843	> 16.7	20.1
^{246}Bk	6.071	> 7.89	9.89
^{249}Md	8.465	< 1.60	0.79
^{251}Md	8.075	>3.38	2.07
^{252}Md	7.985	> 2.44	3.07
^{256}Db	9.475	>0.52	-0.33
^{259}Md	7.112	> 5.65	5.63

^{260}Md	6.945	> 7.68	7.3
^{260}Db	9.365	<0.23	-0.06
^{261}Db	9.225	< 0.56	-0.23
^{262}Rf	8.495	> 2.41	1.3
^{262}Bh	10.215	<-0.89	-1.79
^{269}Db	9.735	1.11	-0.46